(MULTAN) and refined by full-matrix least-squares (SDP). Hydrogens were located on difference Fourier maps and/or placed in chemically reasonable positions (not refined). **Crystal and Refinement Data** ($C_3H_7ClN_2O_6$): M = 202.6, monoclinic, $P2_1/n$; a = 7.802 (2) Å, b = 10.434 (3) Å, c = 9.480 (2) Å, β = 95.79 (2)°; Z = 4; V = 767.8 Å, D_x = 1.751 (2) g cm^{-3}. Of 2889 measured reflections, 1003 were unique (Rint = 0.029); $F(000)$ = 416, R = 0.028, R_w = 0.043 for 873 reflections with $I > 2\sigma(I)$. Final atomic coordinates are given in Table VI (also see the supplementary material paragraph). Relevant bond distances and angles are included in Table V.

Acknowledgment. The support of this research by the National Institute of Environmental Health Sciences (R01 ES 03953) is gratefully acknowledge as are the helpful discussions with Drs. G. J. Gleicher, L. Keefer, C. J. Michejda, and S. R. Koeppke.

Supplementary Material Available: Tables including hydrogen atom positions and anisotropic thermal parameters (1 page); listing of observed and calculated structure factors (5 pages). Ordering information is given on any current masthead page.

An EXAFS Study of Co-Mn/SiO_2 Bimetallic Solvated Metal Atom Dispersed (SMAD) Catalysts

Beng Jit Tan,[†] Kenneth J. Klabunde,*[,†] Tsunehiro Tanaka,[‡,§] Hiroyoshi Kanai,[‡] and Satohiro Yoshida[‡]

Contribution from the Department of Chemistry, Kansas State University, Manhattan, Kansas 66506, and Department of Hydrocarbon Chemistry and Division of Molecular Engineering, Kyoto University, Kyoto 606, Japan. *Received October 15, 1987*

Abstract: Supported cobalt-manganese catalysts prepared by solvated metal atom dispersion (SMAD) were studied by X-ray absorption spectroscopy (EXAFS). The manganese was found to be in the oxidized state, while the cobalt is in both the metallic and oxidized state. Manganese allows an appreciable increase in metallic cobalt present. The XAS results indicate that the most active Co-Mn/SiO_2 catalyst has the largest amount of metallic cobalt and that there is some carbon coordinated to the cobalt atoms. These results are consistent with catalytic data and suggest that Mn scavanges oxygen moieties (which are present in limited amounts) and allows Co to remain metallic. Other possible aiding functions of Mn are also discussed.

In recent years we have reported numerous examples of the synthesis and activities of unusual catalysts prepared by solvated metal atom dispersion (SMAD).[1-6] By this process, metal atoms are solvated at low temperatures in toluene or some other appropriate solvent, and upon warming metal atom clustering begins. This nucleation process (cluster growth) competes with a reaction channel where the growing clusters react with the host solvent. These growing clusters incorporate carbonaceous fragments and are stabilized as amorphous "pseudoorganometallic" powders. These carbonaceous fragments aid in the catalytic reaction and apparently provide a better means of attachment of the metal particles to catalyst support surfaces. Final cluster/particle size can be controlled by length of time of aging at low temperatures, dilution, type of solvent, and by the surface properties of the support used to capture the clusters.

In 1984 we reported the first examples of bimetallic catalysts prepared by the SMAD procedure.[7,8] Of primary interest are the Co-Mn/SiO_2 catalysts. Addition of an equimolar amount of Mn-Co/SiO_2 SMAD catalysts increased the catalytic activity for hydrogenation and hydrogenolysis reactions by 100-fold. A large amount of data on catalytic activity/selectivity showed that the Mn addition greatly affected the activities of Co but not selectivities. Mn itself was catalytically inactive. Extensive chemisorption studies showed that addition of Mn caused an increase in Co dispersion by only 2-fold. Therefore, we tentatively proposed that Mn, in addition to aiding dispersion, also favorably affected catalysis by Co by an electronic effect.

These interesting results prompted us to use extended X-ray absorption fine structure (EXAFS) spectroscopy to obtain information on the local structure surrounding the Co atom from the analysis of the Co and Mn K-edge spectra. The application of EXAFS to the study of catalytic systems and small metal clusters has had considerable impact in the understanding of the structure of these systems.[9-11]

Measurements of EXAFS are particularly valuable for very highly dispersed catalysts. From an analysis of EXAFS data, one can determine the number of neighboring atoms of a particular kind at a particular distance from a given type of absorber atom. By determining EXAFS for each element of interest in a complex material, it is possible to obtain information on the environments of the different types of atoms present. In this paper we report the results of EXAFS studies on the bimetallic SMAD Co-Mn-SiO_2 catalysts.

Experimental Section

Materials. Metals were obtained from Matheson, Coleman, and Bell (Mn) and Cerac, Inc. (Co). The catalyst support was Davison SiO_2 (300 m^2/gm). The support was calcined at 773 K for 3 h in flowing dry air

[†] Kansas State University.
[‡] Kyoto University.
[§] Present address: Department of Chemistry, Faculty of Science, Hokkaido University, Sapporo 060, Japan.

(1) Klabunde, K. J.; Efner, H. F.; Satek, L.; Donley, J. *J. Organomet. Chem.* **1974**, *71*, 309.
(2) Klabunde, K. J.; Efner, H. F.; Murdock, T. O.; Roppel, R. *J. Am. Chem. Soc.* **1976**, *98*, 1021.
(3) Klabunde, K. J.; Ralston, D. H.; Zoellner, R.; Hattori, H.; Tanaka, Y.; *J. Catal.* **1978**, *55*, 213.
(4) Matsuo, K.; Klabunde, K. J. *J. Catal.* **1982**, *73*, 216-227.
(5) Klabunde, K. J.; Tanaka, Y. *J. Mol. Catal.* **1983**, *21*, 57-79, and references therein.
(6) Kanai, H.; Tan, B. J.; Klabunde, K. J. *Langmuir* **1986**, *2*, 760-765.
(7) Klabunde, K. J.; Imizu, Y. *J. Am. Chem. Soc.* **1984**, *106*, 2721-2722.
(8) Imizu, Y.; Klabunde, K. J. *Catalysis of Organic Reactions*; Augustine, R. L., Ed.; Marcel Dekker: New York, 1985; pp 225-250.
(9) (a) Sinfelt, J. H.; Via, G. H.; Lytle, F. W.; Greagor, R. B. *J. Chem. Phys.* **1979**, *71*, 690. (b) Meitzner, G.; Via, G. H.; Lytle, F. W.; Sinfelt, J. H. *Ibid.* **1983**, *78*, 882. Meitzner, G.; Via, G. H.; Lytle, F. W.; Sinfelt, J. H. *Ibid.* **1983**, *78*, 2533.
(10) Asakura, K.; Kosugi, N.; Iwasawa, Y.; Kuroda, H. *EXAFS and Near Edge Structure III*; Springer Verlag: 1984; p 190, and references therein.
(11) Clausen, B. S.; Topsøe, H.; Candia, R.; Villadsen, J.; Leugeler, B.; Als-Nielsen, J.; Christensen, F. *J. Phys. Chem.* **1981**, *85*, 3868.

0002-7863/88/1510-5951$01.50/0

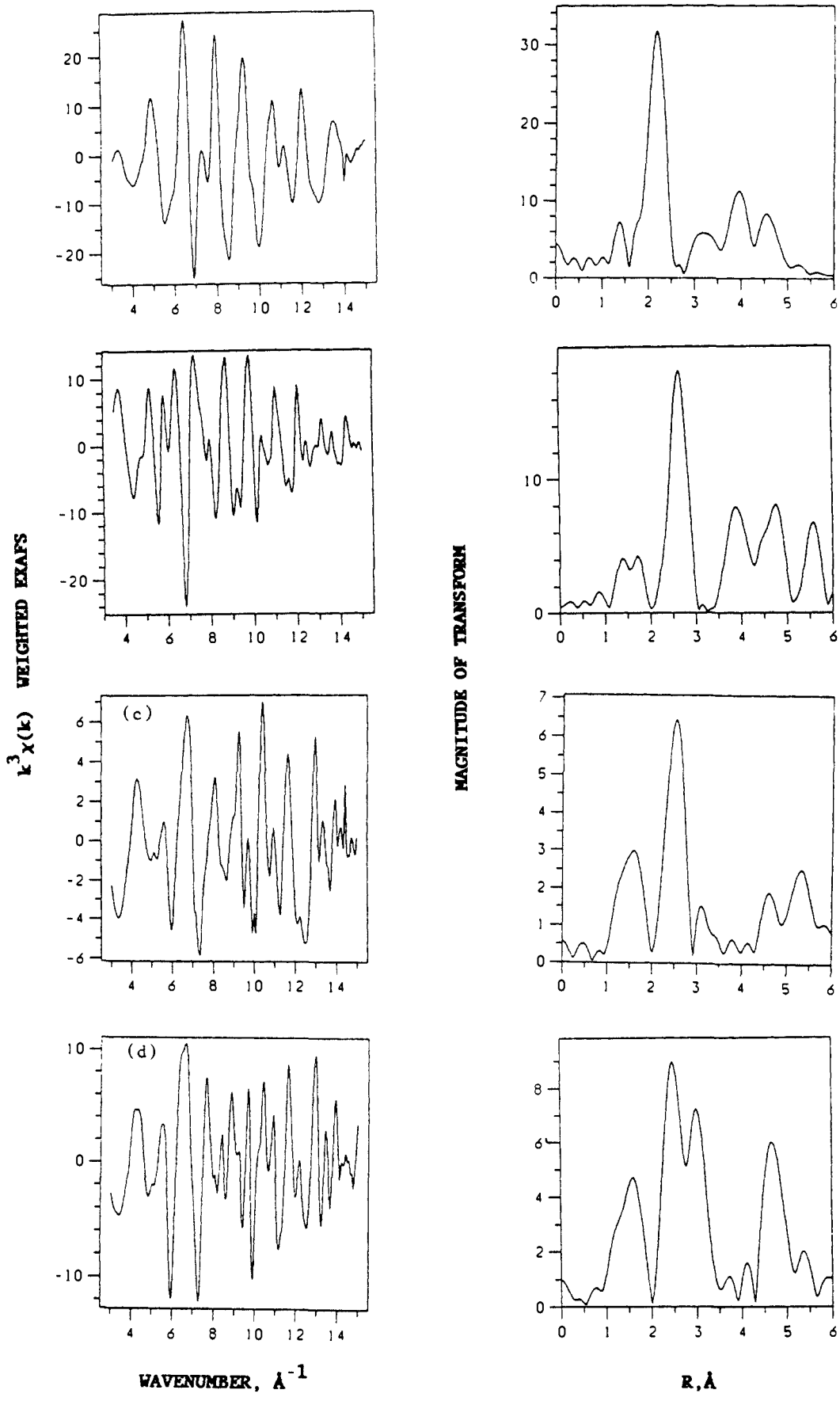

Figure 1. Normalized EXAFS data with associated Fourier transforms for reference Co compounds: (a) cobalt foil (10 μm thick), (b)CoO, (c) $Co(OH)_2$, and (d) Co_3O_4. The EXAFS data are for the extended fine structure beyond the K absorption edge of cobalt.

(420 mL/min) and cooled in flowing N_2 (500 mL/min). Toluene was used exclusively as the metal atom solvation/deposition medium and was purified according to methods described earlier.[5] Commercially available metals, oxides, and hydroxides were used as reference materials: Co foil (The Japan Lamp Industries), CoO (NakaraiChemical Co.), $Co(OH)_2$ (Nakarai Chemical Co.), Co_3O_4 (Nakarai Chemical Co.), and MnO

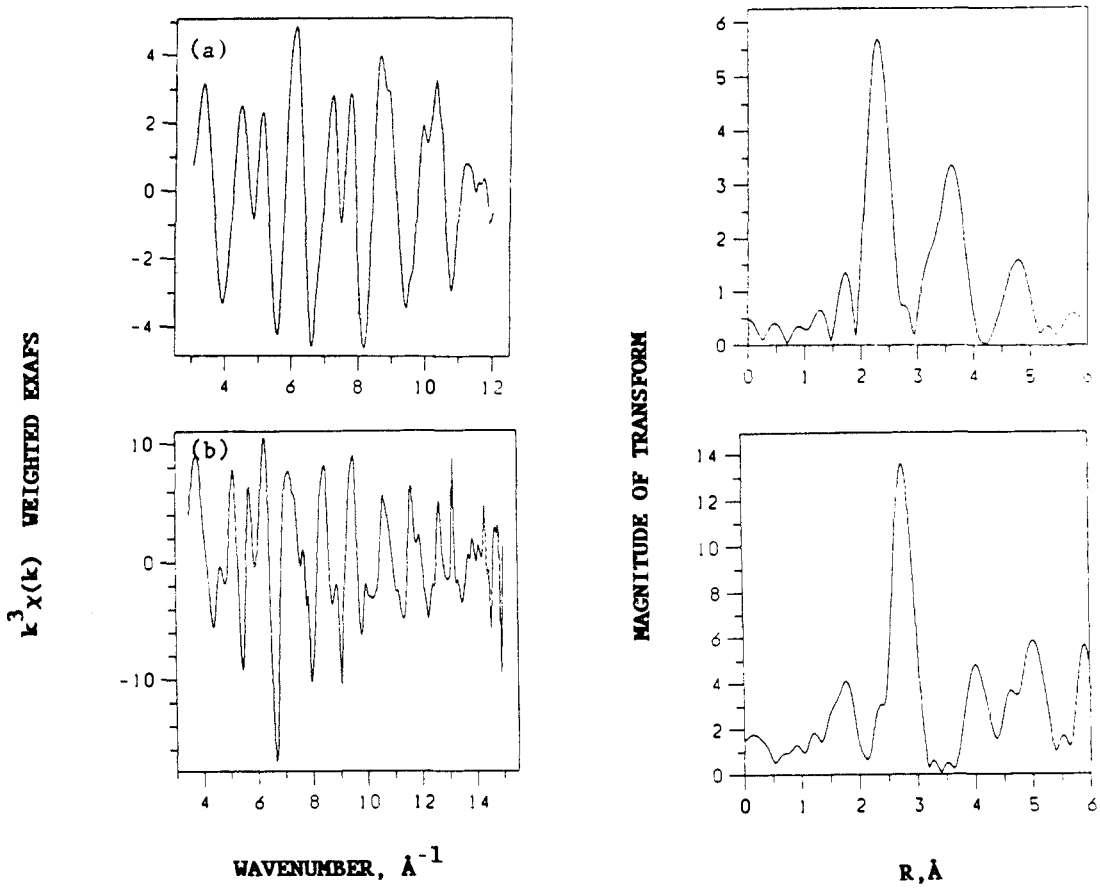

Figure 2. Normalized EXAFS data with associated Fourier transforms for reference Mn compounds: (a) sputtered Mn foil and (b) MnO. The EXAFS data are for the extended fine structure beyond the K absorption edge of manganese.

Table I. Curve-Fitting Data for Standard Co and Mn Compounds[a]

compound	B_j[b]	R,[c] Å	σ^2,[d] Å^2	
Co foil	6.94 (12)	2.49 (2.51)	0.0061	Co–Co
Mn (sputtered)	1.27 (8)	2.64 (2.67)	0.00646	Mn–Mn
Co_3O_4	1.36 (6)	1.83 (1.89)	0.00544	Co^{III}–O
	0.75 (4)	1.95 (1.99)	0.00004	Co^{II}–O
	3.50 (6)	2.86 (2.86)	0.00843	Co^{III}–Co^{III}
	2.43 (6)	3.37 (3.35)	0.00395	Co^{II}–Co^{III}
	2.30 (4)	3.54 (3.50)	0.01265	Co^{II}–Co^{II}
MnO	2.24 (6)	2.15 (2.22)	0.00980	Mn–O
	4.43 (12)	3.12 (3.14)	0.00666	Mn–Mn

[a] The number in parentheses is that of crystallographic data. [b] B_j, apparent coordination number; $B_j = S_j \times N$, S_j, damping factor; N, true coordination number. [c] R, interatomic length. [d] σ, Debye–Waller factor.

(Mitsuwa Chemical Co.). The magnanese metal standard was prepared by sputtering techniques.

Catalyst Preparation. The metal vapor reactor and catalyst preparation methods have been described in previous publications and references therein.[4,5,7,8]

XAS Data Acquisition. X-ray absorption spectra (XAS) data were obtained by use of synchrotron radiation employing the EXAFS facilities at BL-7C of the Photon Factory in the National Laboratory for High-Energy Physics (KEK-PF), Tsukuba, Japan. A Si(111) double crystal was used to monochromatize X-rays from a 2.5-GeV electron storage ring. A mixture of Co–Mn/SiO_2 SMAD catalyst and polyethylene (Merck) was sandwiched between thin polyethylene disks and were pressed into disks of 2-cm diameter. The disks were then sealed between adhesive tapes under nitrogen. The catalyst samples include the following: 3.7% Co/SiO_2, 8.3% Co–1.6% Mn/SiO_2, 5.6; Co–1.4% Mn/SiO_2 and 3.2% Co–3.9% Mn/SiO_2.

In addition to these catalyst samples, XAS data were also obtained from reference materials: Co foil and Mn film; MnO, CoO, $Co(OH)_2$, and Co_3O_4. XAS data were also obtained for conventional catalysts prepared by impregnation of metal nitrates on silica followed by calcination at 773 K and reduction in H_2 at 723 K for 4 h.

All XAS data were taken at room temperature.

Analysis of EXAFS Data. The EXAFS oscillatory part $\chi(E)$ was extracted from the XAS data and normalized as described elsewhere.[12] The photon energy E is expressed in k-space by using the relation

$$k = 2\pi[2m(E - E_0)]^{1/2}/h \quad (1)$$

where m is mass of the electron, h, Planck's constant, and E_0 is the energy threshold which is determined from the position of the inflection points of the absorption edge coefficient.

Plots of the function $k^3\chi(k)$ versus k for the extended fine structure beyond the k-edge are shown on the left-hand side of Figures 1–6. Fourier transforms of these plots are taken over the range of 3.5–12.0 Å^{-1} without phase shift corrections to obtain the radial structure function (RSF) as shown on the right-hand side of these figures. In order to obtain the structure parameters in greater detail, we carried out the curve-fitting procedure. By performing the inverse Fourier transform over the range covering the main peaks of the RSF, we obtain the filtered EXAFS oscillation. The normalized oscillation is represented as a function of k by assuming single scattering[13] and is given by

$$\chi(k) = \sum_j \frac{N_j}{kr_j^2} F_j(k) e^{-2\sigma_j^2 k^2} 3k^2 S_j(k) \sin(2kr_j + \delta_j(k)) e^{-2r_j/\lambda_j(k)} \quad (2)$$

where N_j is the coordination number of scatterers at distance r_j, $f_j(k)$ the backscattering amplitude, δ_j the Debye–Waller factor introduced to estimate the damping of the amplitude by thermal vibration or static disorder. We fitted the filtered EXAFS by using eq 2 with three variables, namely, $B_j(=N_jS_j)$, r_j, σ_j^2, by employing the iterative nonlinear least-squares method of Levernberg.[14] Theoretical phase shifts and backscattering amplitudes of Teo and Lee[15] are used. Table I shows the result of the curve fitting of the reference compounds as examples to check the validity of this method. Bond distances are consistent with those from crystallographic values. Dividing B_j values by coordination numbers, S_j

(12) Tanaka, T.; Yamashita, H.; Tsuchitai, R.; Funabiki, T.; Yoshida, S. *J. Chem. Soc., Faraday Trans. 1*, in press.

(13) (a) Stern, E. A. *Phys. Rev. B* **1974**, *10*, 3027. (b) Ashley, C. A.; Doniach, S. *Phys. Rev. B* **1975**, *11*, 1279. (c) Lee, P. A.; Pendry, J. B. *Phys. Rev. B* **1975**, *11*, 2795.

(14) Levenberg, K. *Quarterly Appl. Math.* **1944**, *2*, 164–168.

(15) Teo, B. K.; Lee, P. A. *J. Am. Chem. Soc.* **1979**, *101*, 2815.

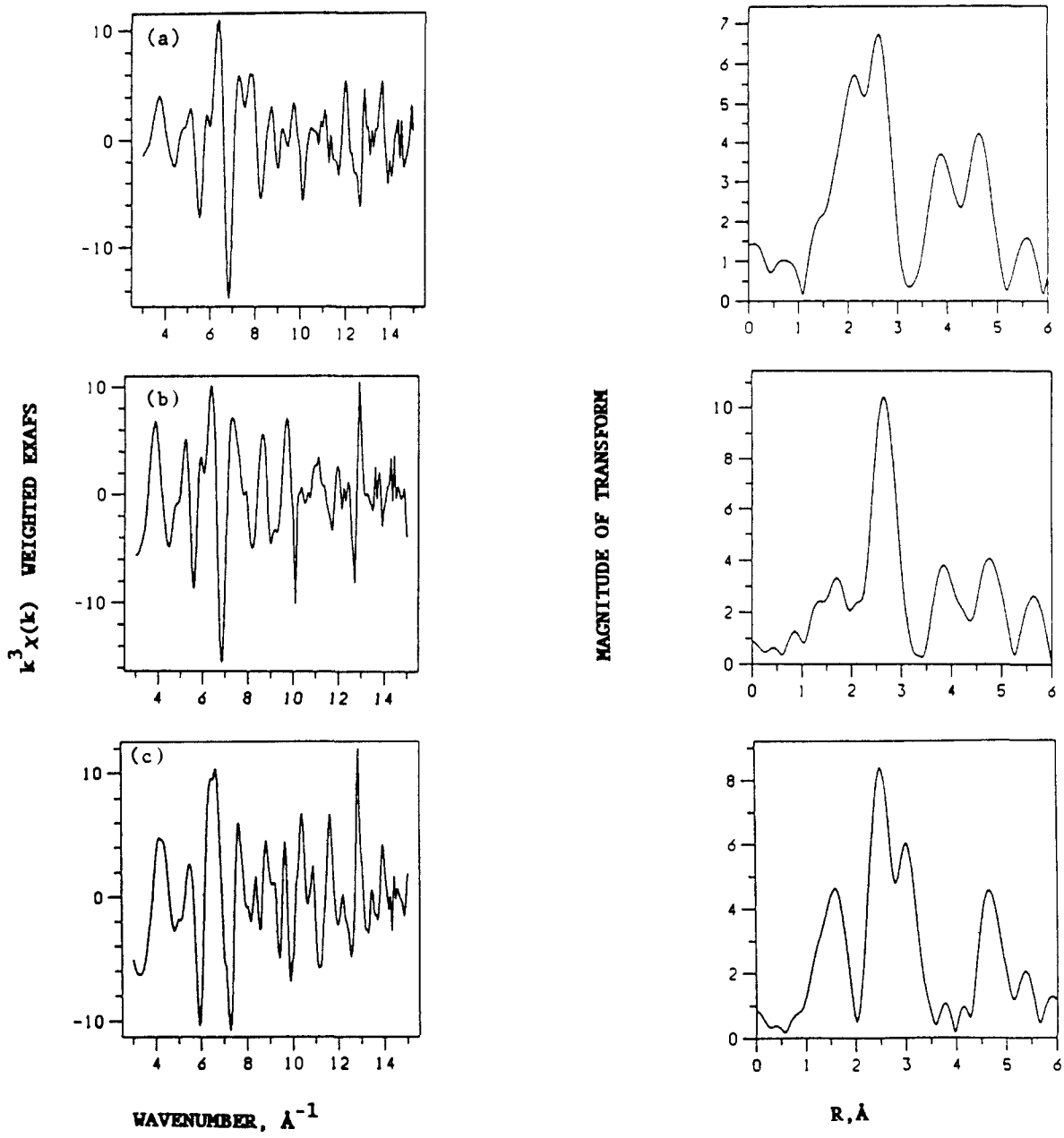

Figure 3. Normalized EXAFS data with associated Fourier transforms for the conventionally prepared catalysts: (a) 5% $CoOx/SiO_2$ (reduced in H_2 at 723 K for 4 h), (b) 5% CoOx–5% $MnOx/SiO_2$ (reduced in H_2 at 723 K for 4 h), (c) calcined 5% $CoOx/SiO_2$ (calcined at 773 K in air for 4 h). The EXAFS data are for the extended fine structure beyond the K absorption edge of cobalt.

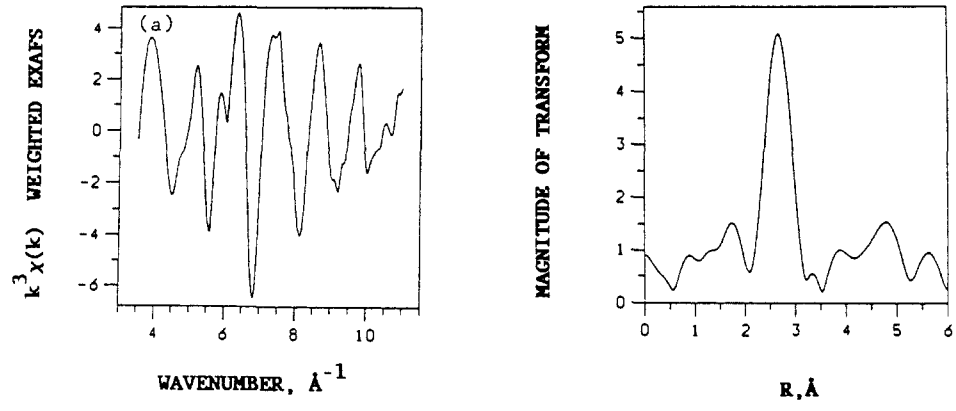

Figure 4. Normalized EXAFS data with associated Fourier transforms for the conventionally prepared catalysts: 5% CoOx–5% $MnOx/SiO_2$ (reduced in H_2). The EXAFS data are for the extended fine structure beyond the K absorption edge of manganese.

is estimated to be approximately 0.5. Although S_j is not strictly a constant, it can be approximated to be a constant.[16] Thus B_j is proportional to the coordination number.

Results

The cobalt–manganese catalysts investigated in this work consist

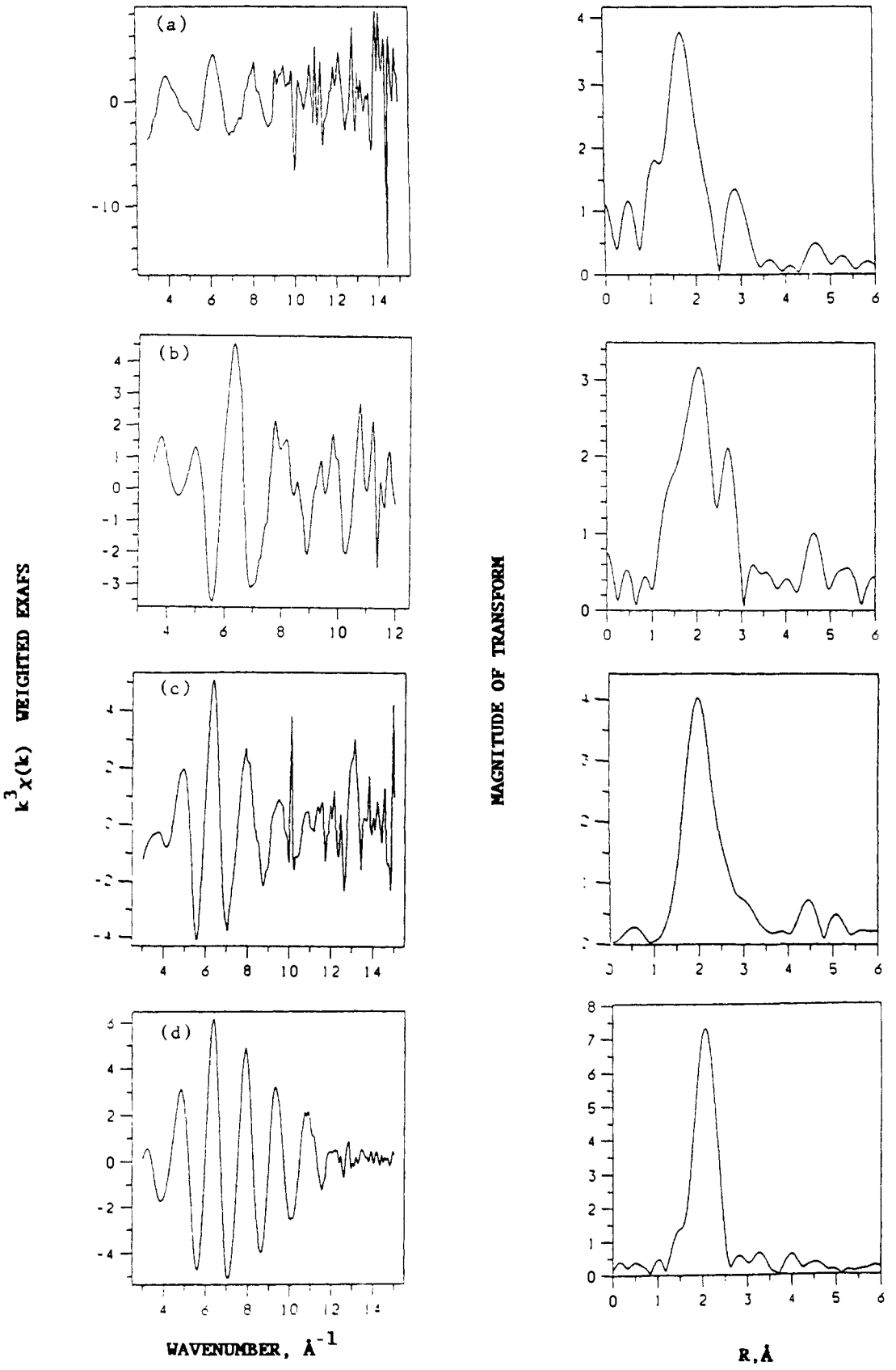

Figure 5. Normalized EXAFS data with associated Fourier transforms for the series of SMAD catalysts: (a) 3.7% Co/SiO_2, (b) 5.6% Co–1.4% Mn/SiO_2, (c) 8.3% Co–1.6% Mn/SiO_2, (d) 3.2% Co–3.9% Mn/SiO_2. The EXAFS data are for the extended fine structure beyond the K absorption edge of cobalt.

of clusters of cobalt and manganese atoms dispersed on silica. Estimates of metal dispersion, defined as the ratio of surface metal atoms to total metal atoms in the clusters, may be obtained from chemisorption data.

We have reported our results for hydrogen adsorption over some $Co–Mn/SiO_2$ in a previous publication.[8] Dispersion was calculated based on 1:1 stoichiometry of hydrogen atoms to surface atoms.[17]

(16) Stern, E. A.; Bunker, B. A.; Heald, S. M. *Phys. Rev. B* **1980**, *21*, 5521.

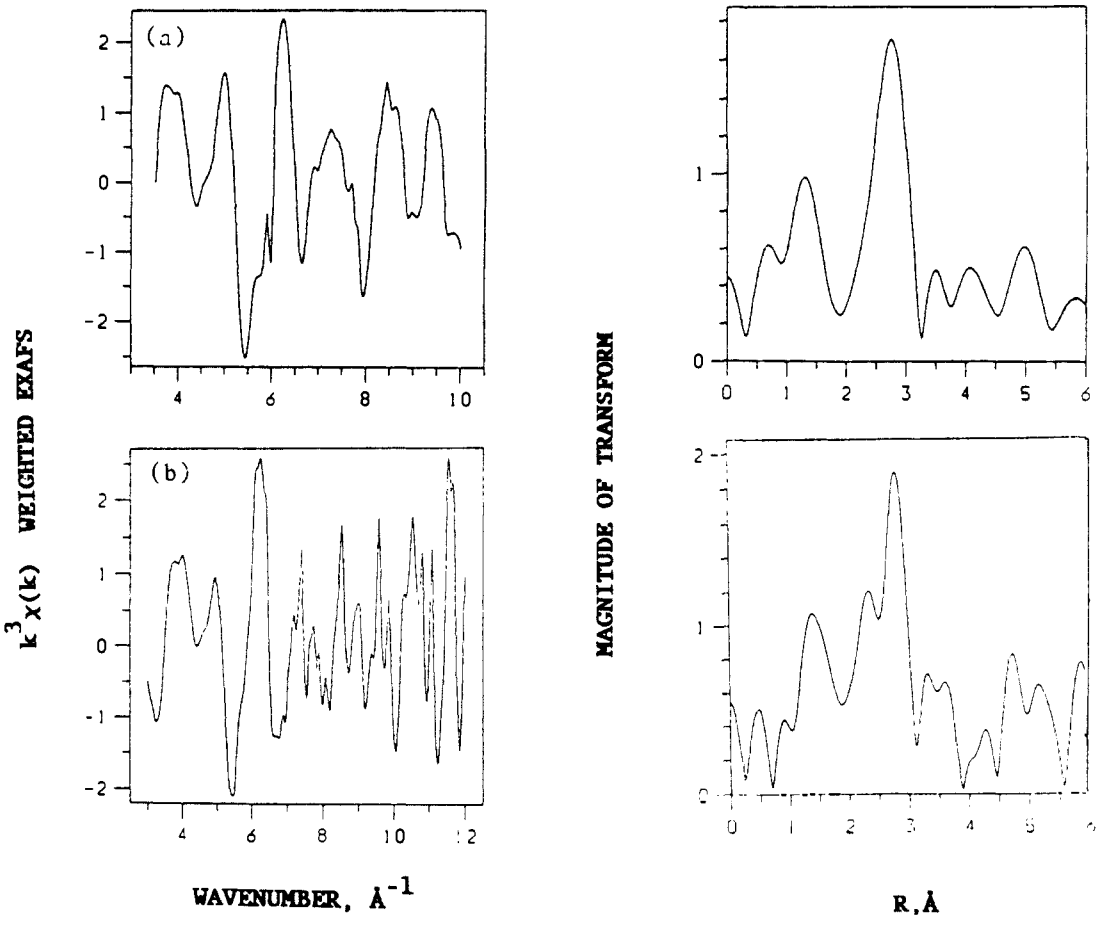

Figure 6. Normalized EXAFS data with associated Fourier transforms for the SMAD catalysts: (a) 3.7% Mn/SiO_2 and (b) 3.9% Mn–3.2% Co/SiO_2. The EXAFS data are for the extended fine structure beyond the K absorption edge of manganese.

Table II. Structural Parameters for $Co–Mn/SiO_2$ Bimetallic Catalysts[a]

	Co–Co		Co–Mn			Co–C		Co–O	
catalyst (Mn/Co)	*B*	*L*	*B*	*L*	B_{Co-Mn}/B_{Co-Co}	*B*	*L*	*B*	*L*
3.7% Co	0.27	2.48				0.13	1.89	1.4	2.01
8.3% Co–1.6% Mn	3.0	2.47	0.51	2.67	0.17	0.25	1.96	0.25	2.01
5.6% Co–1.4% Mn	2.3	2.47	0.24	2.72	0.10	0.33	1.92	0.51	2.04
3.2% Co–3.9% Mn	3.3	2.46	1.2	2.67	0.38	0.32	1.91	0.10	2.03

[a] *B*, apparent coordination number (see text); *L*, interatomic distance.

Dispersion values exceeded 0.5 for $Co–Mn–SiO_2$ and Co/SiO_2. Superdispersion was observed for 3.6% Co–0.8% $Mn–SiO_2$ (having a dispersion of 1.01).

Figure 1 shows the Co K-edge k^3-weighted EXAFS and corresponding RSF of the reference samples, Co metal, CoO, $Co(OH)_2$, and Co_3O_4. The peaks appearing in the region of 1–2 Å in the RSF are due to scattering by neighboring oxygen atoms. Evidently the Co–O pair is not observed in the RSF of the cobalt metal, and the position of the peak due to the Co–Co pair in Co metal is slightly lower than those in Co oxide/hydroxide. Plots similar to Figure 1 are shown in Figure 2 for data obtained for the manganese references samples, namely, Mn metal and MnO. Since we could not obtain a high purity Mn foil, a Mn film prepared by sputtering techniques was used as the standard reference for Mn metal. The Mn metal EXAFS is a little broader, and the peaks of its RSF are of rather low intensity. The peak position of the Mn–Mn pair in the metal is lower than that of the oxide. The structural parameters of the reference samples were well fitted with crystallographic data on the basis of different S_j.

The Co K-edge EXAFS and RSF of the calcined and reduced conventional catalysts, 5% $CoOx/SiO_2$ and 5% CoOx–5% $MnOx/SiO_2$, are shown in Figure 3. The EXAFS oscillations are a little complex for the former catalyst showing the presence of a mixture of metallic Co species and CoO. Note that the RSF of Figure 3a may be produced by superposition of the RSFs of

Table III. Curve Fitting for 3.24% Co–3.98% Mn/SiO_2[a]

	L, Å	*B*	σ^2, Å^2	*R*
Co	2.468	2.8	0.010 67	0.010 67
Co	2.461	3.4	0.011 35	0.001 58
Mn	2.664	3.1	0.028 80	
Co	2.467	2.9	0.010 64	0.011 27
C	1.960	0.9	0.017 65	
Co	2.467	2.8	0.010 68	0.011 12
O	1.887	0.6	0.018 42	
Co	2.468	2.8	0.010 66	
C	1.876	0.3	0.000 00	0.010 35
O	2.003	0.2	0.000 00	
Co	2.463	3.3	0.010 87	
Mn	2.670	1.2	0.017 26	
C	1.906	0.3	0.005 25	0.000 75
O	2.029	0.1	0.000 04	

[a] *L*, interatomic distance; *B*, apparent coodination number; $B = S \times N$, S, damping factor (or amplitude reduction factor); *N*, real coordination number; σ, Debye–Waller factor; *R*, index of the agreement between observed and calculated $\chi(k)$s.

(17) Reuel, R. C.; Bartholomew, C. H. *J. Catal.* **1984**, *85*, 63.
(18) These oxygen moieties may either be from residual oxygen in the vacuum system and/or from the hydroxyl groups of the silica support. Further studies will help us determine the source of these oxygen species.

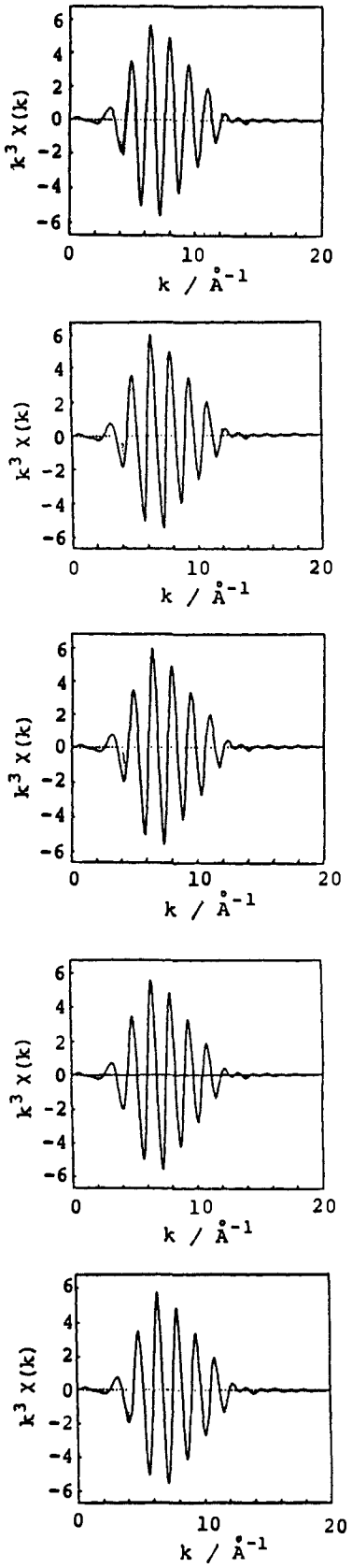

B_j	R / Å	σ / Å^2		R factor
2.84	2.46	0.01067	Co-Co	0.01641
2.82	2.47	0.01068	Co-Co	0.01112
0.57	1.89	0.01836	Co-O	
2.81	2.47	0.01066	Co-Co	0.01035
0.32	1.88	0.00000	Co-C	
0.25	2.00	0.00000	Co-O	
3.06	2.46	0.01087	Co-Co	0.00050
2.60	2.64	0.02870	Co-Mn	
0.38	1.91	0.02267	Co-O	
3.29	2.46	0.01087	Co-Co	0.00075
1.25	2.67	0.01726	Co-Mn	
0.32	1.91	0.00525	Co-C	
0.10	2.03	0.00004	Co-O	

Figure 7. Curve-fitting procedure for the SMAD 3.2% Co–3.9% Mn/SiO$_2$. The figure shows the various ways in which the fitting parameters were used in eq 2 to obtain the best fit for the inverse transform of the EXAFS data for the K-absorption edge of cobalt.

Figure 1 (parts a and b). On the other hand, in the case of CoOx–MnOx/SiO$_2$, the cobalt is mostly present in the CoO state. The cobalt species in the calcined 5% CoOx/SiO$_2$ is found to be Co_3O_4 (compare Figure 3 (parts c and d)). The Mn K-edge

EXAFS and the corresponding RSF of the reduced conventional catalyst, 5% MnOx–5% CoOx/SiO_2, is assigned to be of the MnO structure (Figure 4). There are no appreciable peaks showing any evidence of the presence of Mn in the metallic state.

Figure 5 shows the Co K-edge EXAFS and the RSFs of the SMAD catalysts. Except for Figure 5a, all catalysts contain Co(0), and the most intense peak of each RSF is found at ca. 2 Å. This peak is due to the scattering of the first adjacent Co atoms in Co metal as seen in Figure 1a. The results show that the Co–Mn/SiO_2 SMAD catalysts contain Co in the metallic state. On the other hand, the cobalt species in the 3.7% Co/SiO_2 SMAD catalyst is predominantly in the oxidized state with very small amounts of metallic cobalt. Figure 6 shows the typical Mn K-edge EXAFS and RSF of an Mn SMAD or Co–Mn SMAD catalyst. Judging from the position of the peak due to the Mn–metal atom pair, it can be said that the Mn is in the oxidized state. The peak intensity of the Mn–O pair is low compared to the height of the Mn–metal pair. This does not mean that the coordination number of oxygen atoms around an Mn atoms is small but that there are many kinds of Mn–O bonds. Such phenomena are often observed in complete metal oxides, such as decavanadate, vanadium pentoxide, molybdenum trioxide, etc. Thus, the Co–Mn SMAD catalysts have cobalt in the metallic state as well as the oxidized state, while the manganese is found only in the oxidized state.

Discussion

A study of the Fourier transforms of the Mn K-edge EXAFS of both conventional catalysts (Figure 4) and SMAD catalysts (Figure 6) shows that the Mn species in both these groups of catalysts are in the oxidized state. Mn(0) is not present in the catalysts we have studied so far. This is indeed surprising as the SMAD procedure is carried at low-temperature "reducing environment" consisting of pure toluene and metal under vacuum. Although our ultimate vacuum is crude ($\sim 10^{-4}$ Torr) by UHV standards, and some adventitous oxygen is certainly a potential problem, we believe that the toluene environment (solid/liquid and some vapor) accounts for the vapor pressure in the system. Also, our SMAD procedure often yields highly pyrophoric materials and successfully produces very oxygen-sensitive organometallics.

On the basis of these observations we believe that Mn oxidation must be resulting, at least in part from Mn scavenging of oxygen moieties,[18] from the SiO_2 surfaces.

The Fourier transforms of Co K-edge EXAFS show more interesting results. A study of Figure 3 shows that the reduced conventionally prepared monometallic 5% CoO_x/SiO_2 catalyst has substantial amounts of metallic Co as well as oxidized cobalt species. On the other hand, the predominant Co species in the reduced conventionally prepared 5% CoO_x–5% MnO_x/SiO_2 catalyst is in the oxidized state. The presence of manganese oxides seem to make the reduction of cobalt difficult. The Fourier transforms of the SMAD catalysts (Figure 5) reveal that most of the Co in the 3.7% Co/SiO_2 catalyst is in the oxidized state. However, addition of Mn (Mn/Co = 0.2 mol ratio) inhibits the formation of cobalt oxides. When the ratio of Mn/Co ratio reached a value of 1.3, the Fourier transform of the 3.2% Co–3.9% Mn/SiO_2 indicates that there is a large number of metallic Co–Co bonds showing that essentially all or most of the Co species exists in the metallic state. Interestingly, the most active Co–Mn/SiO_2 catalyst had a Mn:Co ratio of one.[7,8] No peaks are observed above the background noise level of distances greater than 3.5 Å in all the RSF's of Figure 5. Since the peaks in the radial distribution function correspond to the different coordination shells, the Fourier transforms of the Co–Mn/SiO_2 SMAD catalyst seem to suggest that the contributions from the second, third, and fourth coordination shell of Co atoms is small. This indicates that most of the Co metal and/or oxide clusters should be very small (ultrafine particles probably less than 10 Å). The results of the curve-fitting analysis are summarized in Table II. It is difficult to distinguish atoms with close atomic weights from each other (in our case, Mn and Co, C and O). However, we distinguished these atoms by their bond distances e.g., the Co–Mn distance is ca. 0.2 Å longer than the Co–Co distance. The best result in the curve-fitting analysis was obtained only when the contribution of C atoms was taken into account (Figure 7). This indicates that there is at least some coordination between the carbonaceous fragments which originate from the solvent and the Co atoms. The total coordination number of Co in all the SMAD catalysts is rather low. This is not surprising as the cobalt clusters are very small.

The EXAFS data seem to indicate that the SiO_2 surface can provide a significant but limited amount of oxygen. The more oxophilic metal, Mn, may scavenge this oxygen allowing Co to remain in the metallic state. This idea is consistent with our chemisorption data reported earlier.[8]

We still have to rationalize the very large catalytic rate increase even if Mn does allow an appreciable increase in metallic Co present. This may be done through a 2-fold effect of Mn on the Co. The first effect is that Mn allows more Co to be metallic in nature during synthesis of the SMAD catalysts. It also scavenges the oxygen present on the SiO_2 surface and prevents the formation of cobalt oxides on the surface of the Co metal clusters.

Another possible explanation is that the Mn gets interdispersed among the Co and forms a protective partial "coating" around the Co clusters preventing oxygen from reaching the Co metal clusters. The B_{Co-O} drops drastically as the number of nearest neighbor Mn atoms surrounding the Co atom increases (Table II). Note also that though the mol ratio of Mn:Co increased from 0.2 to 0.27 in going from 8.3% Co–1.6% Mn/SiO_2 to 5.6% Co–1.4% Mn, the number of oxygens coordinated to the Co atom increased from 0.25 to 0.51. This is due to the effect of a larger loading of Co in the first catalyst as compared to the latter. The increased Co loading in the 8.3% Co–1.6% Mn/SiO_2 allowed for an increase in the amount of metallic cobalt.

We believe that further EXAFS work and refinement will shed more light on the intimate structure of the Co–Mn particles. Nonetheless, this interesting oxygen-scavenging property of Mn is an important finding and points the way toward the synthesis of further unusual catalysts probably not available by conventional methods.

Acknowledgment. The generous support of the National Science Foundation (to K.J.K.) is greatly appreciated. This work has been performed under the approval of the Photon Factory Program Advisory Committee (proposal no. 86-085).